Afr Archaeol Rev (2021) 38:297–318
https://doi.org/10.1007/s10437-021-09430-0

ORIGINAL ARTICLE

Characterization of Glass, Shell, and Fishbone Beads on Ibo Island (Northern Mozambique) in the Context of the Indian Ocean Trade

Manuel García-Heras · Fernando Agua · Hilario Madiquida · Víctor M. Fernández · Jorge de Torres · María-Ángeles Villegas · Marisa Ruiz-Gálvez

Accepted: 21 February 2021 / Published online: 30 March 2021

Abstract A set of beads made of glass, gastropod mollusk shell, and fishbone from a Swahili occupation level on Ibo Island (northern Mozambique) is dated to the eleventh and twelfth centuries AD. The chemical composition of the glass beads and their chromophores, and the shell and fishbone materials, are studied to understand the local and trading provenance of these items. Representative samples of each material, including two flat glass shards, were characterized using optical microscopy, field emission scanning electron microscopy (FESEM) with energy dispersive X-ray (EDS) microanalysis attached, UV-Vis-NIR spectrophotometry, and X-ray diffraction (XRD). Glass beads represent 60% of the bead assemblage. The shell and fishbone beads are 38.75% and 1.25%, respectively. Three groups of glasses were identified: (1) mineral-soda alumina glass beads associated with the recently identified m-Na-Al 6 group that come from Western India; (2) vegetal-soda alumina, represented by one flat glass shard probably from the Middle East, and beads of v-Na-Al glass of type A that came from Central Asia; and (3) conventional soda-lime silicate glasses, of modern chronology and probable European origin. Groups 1 and 2 show a variety of chromophores, both ionic and colloidal. A ruby-color bead was also identified as belonging to the Na_2O-ZnO-SiO_2 system and colored with cadmium sulfoselenide colloids, but this was of modern chronology. Shell beads were made from *Lambis lambis* gastropod mollusk shells and were locally produced. The fishbone beads may have been from a cartilaginous fish of the Chondrichthyes class, but it is difficult to specify the taxonomical level. The results of the analysis suggest that Ibo Island was integrated very early into the Swahili trade networks of the Indian Ocean.

Résumé Un ensemble de perles en verre, coquille de mollusque gastéropode et arête de poisson provenant d'une occupation Swahili dans l'île d'Ibo (nord du Mozambique) est daté des 11ème et 12ème siècles après JC. La composition chimique des perles de verre et leurs chromophores, ainsi que les matériaux en coquille et en arête de poisson, sont étudiés pour comprendre la provenance locale ou commerciale de ces objects. Des échantillons représentatifs de chaque matériau, y compris deux éclats de verre plats, ont été caractérisés par microscopie optique, microscopie électronique à

M. García-Heras (✉) · F. Agua · M.-Á. Villegas
Institute of History, Spanish National Research Council (CSIC), Madrid, Spain
e-mail: manuel.gheras@cchs.csic.es

H. Madiquida
Department of Archaeology and Anthropology, Eduardo Mondlane University, Maputo, Mozambique

V. M. Fernández · M. Ruiz-Gálvez
Department of Prehistory, Ancient History and Archaeology, Complutense University, Madrid, Spain

J. de Torres
Institute of Heritage Sciences, Spanish National Research Council (CSIC), Santiago de Compostela, Spain

balayage à émission de champ (FESEM) avec microanalyse à rayons X à dispersion d'énergie (EDS) attachée, spectrophotométrie UV-Vis-NIR et diffraction des rayons X (XRD). Les perles de verre représentent 60% de l'ensemble, tandis que les perles de coquille (38,75%) et d'arêtes de poissons (1,25%) représentent le reste. Trois groupes de verres ont été identifiés: 1) des perles d'alumine de soude minérale associées au groupe m-Na-Al 6 récemment identifié qui proviennent de l'Inde occidentale; 2) unéclat de verre plat d'alumine de soude végétale et alumina, probablement du Moyen-Orient, et des perles de verre v-Na-Al de type A provenant d'Asie centrale; et 3) des verres conventionnels de silicate sodo-calcique, de chronologie moderne et probablemente d'origine européenne. Les groupes 1 et 2 ont montré une variété de chromophores, à la fois ioniques et colloïdaux. Une perle de couleur rubis a été également identifiée comme appartenant au système Na_2O-ZnO-SiO_2 et colorée par des colloïdes de sulfoséléniure de cadmium, mais celle-ci etait de la chronologie moderne. Les perles de coquillages ont été fabriquées à partir de coquilles de mollusques gastéropodes *Lambis lambis* et ont été produites localement. Les perles en arête de poisson peuvent provenir d'un poisson cartilagineux de la classe des *Chondrichthyes*, mais il est difficile de préciser le niveau taxonomique. Les données et contextualisation qui en résultent suggèrent que l'île d'Ibo a été intégrée très tôt dans les réseaux commerciaux swahili de l'océan Indien.

Keywords Mozambique · Swahili · Glass beads · Chemical composition · Trade networks

Introduction

Kenya and Tanzania have been the focus of historical, anthropological, and archaeological research projects on the Swahili culture since the end of the nineteenth century (see Wynne-Jonnes and LaViolette 2018). Mozambique, which lacks large stone urban centers, has been considered a marginal area of the Swahili world. As a result, it has received little research attention relating to Swahili archaeology. The civil war that followed independence, lasting until 1992, severely constrained field research. This was especially true for northern Mozambique, the main theater of the civil war. In the mid-1970s, the Eduardo Mondlane University, based in Maputo, started an ambitious archaeological research program throughout the country (Duarte and Meneses 1996; Morais 1988; Sinclair 1985, 1987, 1991; Sinclair et al. 1987). Despite this program, the only systematic and long-term research undertaken on the Swahili has been in Chibuene in central Mozambique (Bandenhorst et al. 2011; Ekblom and Sinclair 2018; Sinclair et al. 2012; Wood et al. 2012). Nevertheless, some areas associated with the Swahili culture in northern Mozambique have also been investigated by members of Mondlane University. In this regard, the studies by Duarte (1993) and Madiquida (2007) offer an overview of the Swahili culture in the Quirimbas archipelago and some coastal sites on the opposite shore.

The construction of a liquified natural gas pipeline in northern Cabo Delgado province brought about an environmental and archaeological impact assessment project. Within this framework, Adamowicz (2011, 2013) conducted field research in a wide area of the Palma district, close to the Tanzanian border and seat of the Swahili Tungi sultanate. As a result, more than thirty Swahili archaeological sites, some of them with stone building remains, were identified. However, no systematic excavation was undertaken in any of them. In summary, research in northern Mozambique has been sporadic and based on small test pits rather than on long-term, horizontal excavations. Radiocarbon dates are thereby scarce, and no archaeometric studies have been accomplished. These have resulted in treating Mozambique, especially its northern shore, as a marginal area of Swahili culture in contrast to Tanzania and Kenya. For this reason, the only Mozambican site mentioned in a recent handbook on the Swahili world is Chibuene (Wynne-Jonnes and LaViolette 2018).

Previous archaeological surveys and test excavations in Ibo, Quisiva, Quirimba, Macaloe, Vamizi, and Matemo confirmed the importance of the Quirimbas archipelago in the study of Swahili culture in northern Mozambique (Duarte 1993; Madiquida 2007; Sinclair 1987). Hence, in cooperation with Eduardo Mondlane University in Maputo, a Spanish archaeological team started a research project in the Quirimbas Islands in 2015. This project's primary goals were to document this region's role as a part of the Swahili cultural and trading networks. After some preliminary results (de Torres et al. 2016), archaeological fieldwork focused on Ibo Island involved conducting a survey and four test excavations. In the fourth test pit, C-400, an in situ living floor was discovered. The excavation of this unit

was expanded during 2016 and 2017 (Ruiz-Gálvez 2020; Ruiz-Gálvez et al. 2017).

A set of glass, shell, and fishbone beads was unearthed, along with other artifacts, in the unit. Two shards of flat glass were also retrieved from the same unit. An archaeometric characterization of the glass artifacts was undertaken to determine the chemical composition of the glass beads and the two shards of glass and define their chromophores. The chemical and mineralogical composition of the shell and fishbone beads was also undertaken. These analyses were carried out to shed new light on the technology and probable trading provenance of these items. With the exception of beads found in Chibuene (Wood et al. 2012), no other beads from Swahili contexts in Mozambique have been previously analyzed with instrumentation, even though similar beads have been commonly found at archaeological sites of eastern and southern Africa (Robertshaw et al. 2006, 2010; Wood 2012). Therefore, this study may fill the gap in the archaeology of the Swahili culture in northern Mozambique and the archaeology of glass in East Africa. It may also provide new insights into the Quirimbas archipelago's role in the complex network of the Indian Ocean trade.

Archaeological Background

The Quirimbas archipelago is located in the Cabo Delgado province, northeastern Mozambique, near the border with Tanzania. It consists of approximately 50 islands made up of coral formations with sand beaches and mangroves. Ibo is the most important island and the capital of the Quirimbas archipelago (Fig. 1). Portuguese chronicles described the Quirimbas Islands as an active area in the Swahili trade and a thriving textile production center. According to Newitt (1995), the islands of Kilwa and Zanzibar in Tanzania, the main Swahili ports, shared close ties with the Quirimbas. Portuguese chronicles mentioned them as active locales in the gold trade between the Zambezi area and the Kilwa sultanate. In fact, in the early sixteenth century AD, the Portuguese attacked the Quirimbas archipelago to control the profitable ivory and gold trade. They then settled on the Quirimbas Islands in 1590. From 1820, Ibo Island became a port of embarkation for enslaved Africans taken to Brazil, Cuba, and French colonies (Palmer and Newitt 2016).

The stratigraphy of the C-400 site, the focus of this study, consisted of an occupation floor about 1.5 m below the surface. Its upper layers (SU 401 and 402) were interpreted as the rubble that originated from the construction of the nearby eighteenth-century Portuguese fort. Fragments of local pottery, shell, and glass beads and fragments of Chinese porcelain and European earthenware were found in the rubble, indicating that part of a Swahili settlement was destroyed in order to erect the Portuguese building. Below the rubble is a layer of sterile white sand (SU 403), possibly a dune, which partially sealed a much older archaeological living floor (SU 405) and helped preserve them from erosion. This level is characterized by dark, organic-rich soil and contained plenty of archaeological and organic materials. The excavation of this layer, about 20 cm thick, revealed several activity areas, including an almost square-shaped hearth, 90 × 84 cm, reddish in color, compact with some charcoal nuggets, and 4–5 cm in thickness (SU 408, Fig. 2: 1). Surrounding the hearth was a structure, 12 cm thick and 40 cm wide, made of a cemented litter of shells, bones, ceramic sherds, beads, and bronze fragments. Even some bronze coins were found in this matrix. The feature offered an almost semicircular design in the center of the excavation, with two negative imprints of postholes (Fig. 2: 2–3). The refuse accumulated on the lower edges of the wooden walls inside a structure. Although the structure's original shape is difficult to estimate due to post-depositional weathering processes, it roughly occupies an area of 11 m^2. Despite its modest size, it is the first site where an in situ occupation floor has been documented in this part of the country (Ruiz-Gálvez et al. 2017).

More than 100 kg of shells and fishbones were recovered during excavation. Otherwise, material culture is dominated by local hand-made pottery with impression, incision, and roulette as the most characteristic decorative techniques. An impressive number of spindle-whorls were unearthed, consistent with the Portuguese chronicles describing the archipelago as a textile production center. Several sherds of imported ceramic wares, some of them glazed, were also recovered (de Torres et al. 2016; Ruiz-Gálvez et al. 2017). Lead and alkaline compositions identified in most of these glazes are technologically compatible with the so-called Samarra glazes produced in the Middle East (García-Heras et al. 2019; Hill et al. 2004). Metallic artifacts were also unearthed, comprising an iron arrow, some fragments of a small bronze chain or necklace, and three

Fig. 1 Location of the Ibo Island in the Cabo Delgado province, northeastern Mozambique (Swahili sites are marked with black dots)

coins, one of which was used as a pendant and is currently being studied with lead isotope analysis. The artifact assemblage also includes two shards of flat glass and a set of beads made of glass, shell, and fishbone.

The assemblage of materials documented in the Swahili living floor indicates a date of the eleventh and twelfth centuries AD. The two AMS dates (1011–1164 cal AD, 1062–1212 cal AD), obtained from the remains of tortoise scapulae, broadly match the chronology provided by the imported ceramics (Fig. 3). The total number of beads recovered by dry sieving was 240, a small number compared to the volume of beads recovered in other more prominent and contemporaneous Swahili towns such as Shanga, Manda, and Kilwa (Wood 2018). Table 1 shows the distribution of beads and flat glass shards through the stratigraphic sequence. One hundred beads (41.66 % of the total) came from the upper and disturbed layers (SU 401,

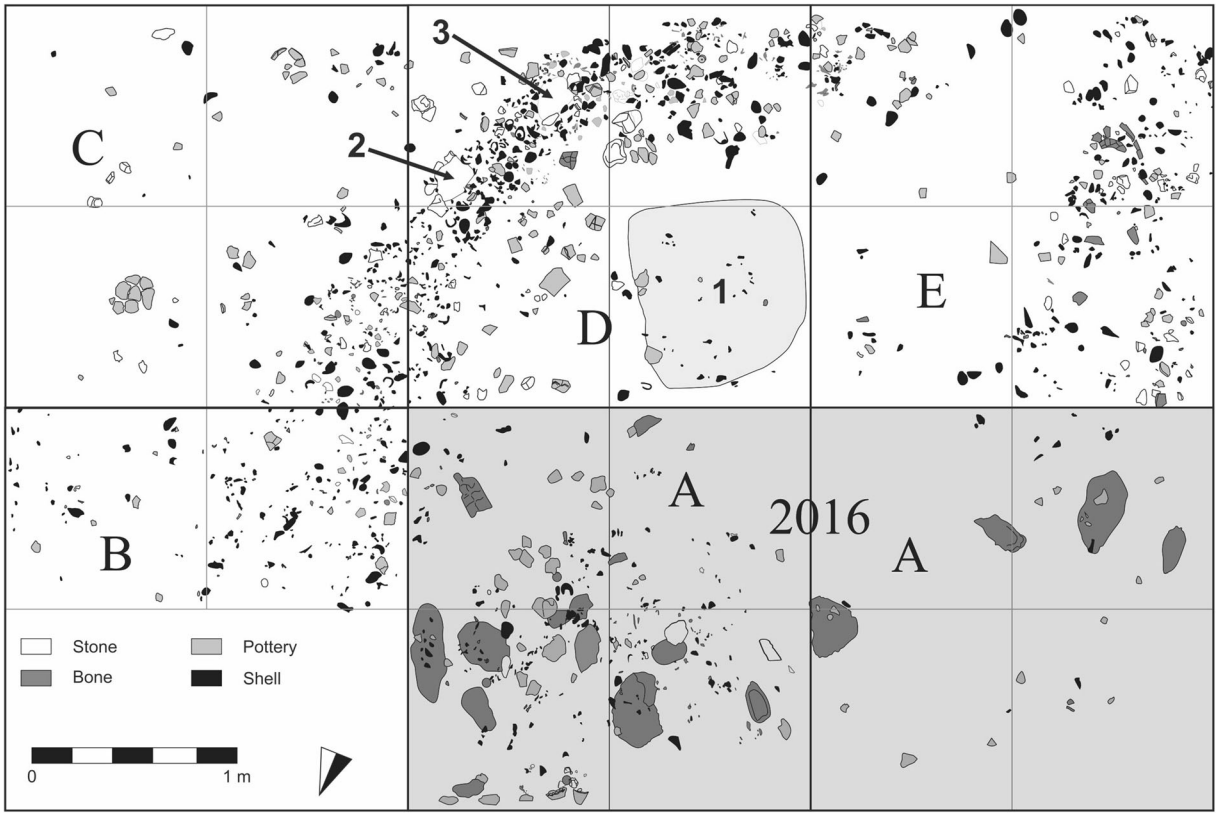

Fig. 2 The C-400 site—activity areas of the black soil layer: 1. almost square hearth; 2–3. negative imprints of postholes

403, and 403C), while the remaining 140 (58.34 % of the total) were retrieved from the living floor area.

Samples Selected and Analytical Techniques

Glass beads accounted for 60% of the beads, and the remaining 40% consisted of shell and fishbone beads. Twelve samples of glass, two shell beads, and one fishbone bead were used in the analysis. The glass samples were selected based on shape and color. These included mostly opaque, some translucent, and very few transparent beads, and mainly cylindrical, spherical, and ellipsoidal shaped. Two shards of flat glass were also selected (MO-6 and MO-8). All the samples are described in Table 2, and their images are shown in Fig. 4. Samples were observed and analyzed using the following techniques: optical microscopy (OM), field emission scanning electron microscopy (FESEM) with energy-dispersive X-ray (EDS) microanalysis attached, UV-Vis-NIR spectrophotometry, and X-ray diffraction (XRD). These techniques have been used to characterize glass materials from different areas of the world (see Agua et al. 2017; García-Heras et al. 2005; Koleini et al. 2019).

OM observations were accomplished with a Motic SMZ 168 microscope, and images were recorded with a Moticam 2500 digital camera. Examination of samples by FESEM was carried out on the surface of samples and polished surfaces and fractures. Observations were also made on embedded and mirror-polished sections using an epoxy resin and an aqueous suspension of cerium oxide. Samples were sputter-coated with graphite on a JEOL JEE4b vaporizer to make them conductive. The equipment used was a Hitachi S4800 cold cathode field emission scanning electron microscope, working with acceleration voltages of 7 and 15 kV. Micrographs were obtained using the secondary electrons (SE) mode. EDS microanalysis was undertaken with a 20 mm^2 Oxford X-Max EDS system, with a resolution of 125 eV (Mn Kα) coupled to the mentioned microscope. The chemical composition of glass samples was estimated using an average of three measurements carried out on the polished sections. The EDS system

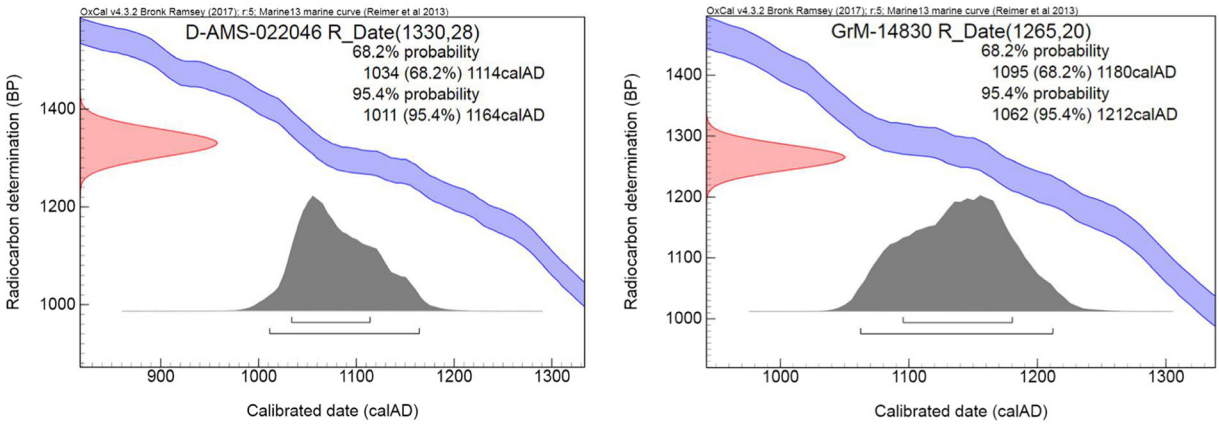

Fig. 3 AMS radiocarbon dates obtained on tortoise scapula

employed is routinely calibrated against pure metals and synthetic standards.

Furthermore, the quality of data was checked against two certified glass reference materials provided by The Society of Glass Technology (Sheffield, UK): Standard Glass No. 7 (soda -lime silicate glass) and Standard Glass No. 10 (amber soda-lime silicate glass). Both certified glass materials were mounted in cold-setting epoxy resin and then mirror-polished using an aqueous suspension of cerium oxide, in the same way as the glass samples analyzed. They were also sputter-coated with graphite. The error or coefficient of variation for major oxides range about 0.20% for SiO_2, 0.79–0.95% for Na_2O, and 1.63–2.08% for CaO, while minor oxides range 6.09–10.69% for MgO, 9.91-11.78% for K_2O, 6.50–11.55% for Al_2O_3, and about 11.50% for Fe_2O_3 (see Tables S1 and S2 in Online Supplementary Materials—OSM). Other oxides such as PbO, MnO, and ZnO, not covered by the aforementioned standards, were routinely measured with the EDS system. The results show coefficients of variation lower than 1.00% for PbO and around 8.00% for MnO and ZnO. The error for Cl^- is in the range of 5.50%.

XRD was carried out in the three selected samples of shell and fishbone to determine their crystalline phases and ascertain their material component. This was accomplished with a PANalytical X'Pert MPD diffractometer, using Kα of copper radiation (1.54056 Å) and working conditions of 45 kV of voltage and 40 mA of intensity. Diffractograms were recorded between 2θ= 5–60°, with an angle step of 0.03°, and a time per step of 2 s. Analyses were made on powder samples grounded with an agate mortar. Finally, chromophores were determined by using UV-Vis-NIR spectrophotometry in those glasses big enough for the analysis. An Ocean Optics HR 4000 CG equipment was used. Spectra were acquired by reflection and recorded in the range of 200 to 1100 nm.

Chemical Composition of Glass

Table 3 shows the results of chemical composition derived from the 12 samples of glass: 10 beads and two shards. Of the 12 glass samples, 11 were made with soda-lime silicate glass from the Na_2O-CaO-SiO_2 system. One piece (MO-11) was made with a glass in which zinc oxide, rather than calcium oxide, was used as a stabilizer and, therefore, belongs to the Na_2O-ZnO-SiO_2 composition system. The Na_2O-ZnO-SiO_2 glass system is nowadays characterized by a percentage of ZnO that does not exceed half of all the alkaline oxides (Bamford 1977; Fernández Navarro 2003). The chemical composition of this sample meets this proportion since the ZnO concentration (8.0 wt. %) does not exceed half of the joint concentration of Na_2O (20.1) + K_2O (4.3) = 24.4 wt. %. Both the compositional data of this bead and the fact that it comes from the upper layers of the unit suggest that it is a modern glass bead. The 11 soda-lime silicate glasses can be divided into three groups:

Group 1 (Table 3) consists of the following six samples (all of them beads): MO-01, MO-07, MO-09, MO-10, MO-12, and MO-15. The content of Na_2O is 18.6–21.0 wt. %; CaO: 1.7–3.6 wt. %; and SiO_2: 62.0–64.7 wt. %. It is characterized by a very low MgO concentration that is barely detected (samples MO-01 and MO-12) or reaches 1.4 wt. %, the highest level (sample MO-07), while Cl^- is between 0.9 and 2.0 wt. %, suggesting that glasses from this group were made from an alkaline raw

Table 1 Distribution of beads and flat glass shards through the stratigraphic sequence

Stratigraphic unit (SU)	Beads			Flat glass
	Glass	Shell	Fish	
401 (disturbed superficial layer)	14 (1 turquoise blue + 1 bluish green +1 green + 1 colorless greenish +7 brick red +3 dark)	19 + 1 tubular fragment of raw shell	1	
403 (white sand dune)	55 (28 brick red + 15 green + 4 yellowish + 8 dark)	9		1 (colorless)
403C (white sand dune)	1 (bright red)			
404 (interface between the sand dune and the Swahili living floor)	13 (9 brick red + 3 dark green, one of them fragmented, + 1 dark fragmented)	13 + 1 tubular fragment of raw shell		1 (colorless bluish)
405A (Swahili living floor inside the structure)	3 (1 green + 2 brick red)	1	2	
405B (Swahili living floor inside the structure)	7 (4 brick red + 2 bluish green + 1 dark)	4		
405D (Swahili living floor inside the structure)	10 (5 brick red + 3 turquoise blue + 1 dark + 1 dark yellow)	8		
405E (Swahili living floor inside the structure)	1 (brick red)	5		
407B (Swahili living floor outside the structure)	2 (brick red)			
407C (Swahili living floor outside the structure)	7 (3 brick red + 4 bluish green)	14 (1 of them bitruncated and of big size)		
407C-D (Swahili living floor outside the structure)	6 (3 brick red + 2 green + 1 yellow)	1		
409B (Refuse deposit inside the structure)	9 (5 brick red + 2 bluish green + 1 dark yellow + 1 dark (probably burned)	11		
409C (refuse deposit)	3 (brick red)	1		
409D (refuse deposit)	4 (2 brick red + 2 bluish green)	1		
409E (refuse deposit)	1 (greenish blue) in the same line			
410B (Rubbish dump outside the structure)	8 (4 brick red +2 bluish green + 1 dark yellow + 1 dark fragmented)	2		
412ABCD (dark soil beneath a shell cluster in the junction of ABCD quadrants)		2		
Total 240 beads + 2 flat glass shards	144	93	3	2

material of mineral origin. According to variations in the contents of Al_2O_3 and K_2O, mineral-soda glasses are separated into natron glasses and soda-alumina glasses. Natron glasses are usually characterized by contents of Al_2O_3 <4.0 wt. % and K_2O <1.5 wt. % and are known in the Middle East until the ninth century AD (Brill 2001; Henderson et al. 2004), whereas contents of both oxides in soda-alumina glasses are higher: up to near 10.0 wt. % of Al_2O_3 and >1.5 wt. % of K_2O (Dussubieux et al. 2010). This second type was first recognized in Indian glasses by Brill (1987) and is very common in Indian and southeastern Asian sites from the fourth century onwards. The beads of this type are widely found in eastern and southern African sites dating from the eighth century AD (Robertshaw et al. 2010). Samples of this group contain high percentages of alumina, which has concentrates of 7.5–8.9 wt. %. Therefore, it deals with mineral-soda alumina glasses. In some parts of present-day India, glassmakers use an evaporite deposit of mineral soda containing high percentages of Na salts as a flux (Brill 1999, 2001; Robertshaw et al. 2010).

Group 2 is composed of four samples (three beads and a colorless flat glass): MO-02, MO-05, MO-06, and MO-14 (Table 3). The Na_2O content is 16.7–20.4 wt. %; CaO: 3.5–5.0 wt. %; and SiO_2: 58.7–67.0 wt. %. The group is characterized by a relatively high MgO concentration (4.7–5.4 wt. %), while Cl^- is somewhat lower than in group 1 (0.9–1.3 wt. %), which suggest that glasses from this group were made from an alkaline raw material of

Table 2 Description of the samples selected for analysis

Sample	Type	Color	Optic	Shape	Material	Level
MO-01	Bead	Bluish-green	Translucent	Cylindrical	Glass	Upper layers
MO-02	Bead	Colorless greenish	Wound opaque	Spherical	Glass	Upper layers
MO-03	Bead	Black	Opaque	Disk-shape	Fishbone	Upper layers
MO-04	Bead	Light gray	Opaque	Disk-shape	Shell	Upper layers
MO-05	Bead	Brick red	Opaque	Cylindrical	Glass	White sand dune
MO-06	Flat glass	Colorless	Transparent	Unknown	Glass	White sand dune
MO-07	Bead	Black	Opaque	Spherical	Glass	Interface dune/living floor
MO-08	Flat glass	Colorless bluish	Transparent	Unknown	Glass	Interface dune/living floor
MO-09	Bead	Brick red	Opaque	Ellipsoidal	Glass	Interface dune/living floor
MO-10	Bead	Green	Transparent	Barrel	Glass	Living floor inside the hut
MO-11	Bead	Ruby red	Opaque	Cylindrical	Glass	Upper layers
MO-12	Bead	Dark yellow	Opaque	Cylindrical	Glass	Living floor inside the hut
MO-13	Bead	Pale ochre	Opaque	Biconical	Shell	Living floor outside the hut
MO-14	Bead	Yellow	Opaque	Spherical	Glass	Living floor outside the hut
MO-15	Bead	Greenish blue	Opaque	Cylindrical	Glass	Refuse deposit

plant origin, probably ashes derived from halophytic plants. In this case, alumina percentages are lower (2.7–5.3 wt. %) than in group 1. These glasses, known in the literature as plant-ash glasses, have been widely found in eastern and southern African sites of the thirteenth to seventeenth centuries AD, and in southern and central Asia, ninth to fourteenth centuries AD (Siu et al. 2020).

Group 3 consists of a single flat glass sample: MO-08 with Na_2O content (15.3 wt. %) that is lower than in the previous two groups (Table 3). Concentrations of CaO (9.0 wt. %) and SiO_2 (71.6 wt. %) are the highest of all glasses analyzed. It is also a glass without MgO or K_2O, and with 3.0 wt. % of alumina. This chemical composition is very close to that of a conventional soda-lime silicate glass made with synthetic soda, especially with an alumina content below 4 wt. %, and is very likely to be of European production. Quite similar compositions have been reported for some European beads found in southern Africa during the late nineteenth century (Koleini et al. 2020).

Color of Glasses and Characterization of Chromophores

Mineral-soda alumina glasses from group 1 show various chromophores that originated from either ionic or colloidal procedures. The greenish blue of the MO-15 and the dark yellow of the MO-12 samples, with 1.5 and 1.8 wt. % of Fe_2O_3, respectively (Table 3), are due to the presence of Fe^{2+}/Fe^{3+} ions and its redox equilibrium, which results in a chromatic sum of the colors imparted by Fe^{2+}ions (blue) and Fe^{3+}-ions (yellow). If there is a higher presence of Fe^{2+}ions, the chromatic sum will tend towards a bluish hue (the case of MO-15), whereas if the higher presence is of Fe^{3+}ions, the chromatic sum will tend towards a more yellowish hue (the case of MO-12) (Bamford 1977; Fernández Navarro 2003). Apart from the presence of the Fe^{2+}/Fe^{3+} redox pair, the bluish-green of MO-01 (Fe_2O_3 = 1.5 wt. %) and the green color of MO-10 (Fe_2O_3 = 3.5 wt. %) are also due to the presence of Cu^{2+}ions, as is shown in Fig. 5. The absorption reflection spectrum shows two very wide bands. The first one is the displacement of the absorption edge up to approximately 450 nm, which imparts a yellow color and can be assigned to Fe^{3+}ions. The second one appears at around 800 nm, which imparts a blue color and can be assigned to the presence of Cu^{2+}ions. Iron oxide was detected in both samples; however, copper oxide was not since, in all probability, it is below the detection limits of the EDS spectrometer used for the analysis. Although an absorption spectrum could not be undertaken, the black color of MO-07 may be due to its high percentage of Fe_2O_3 (2.7 wt. %).

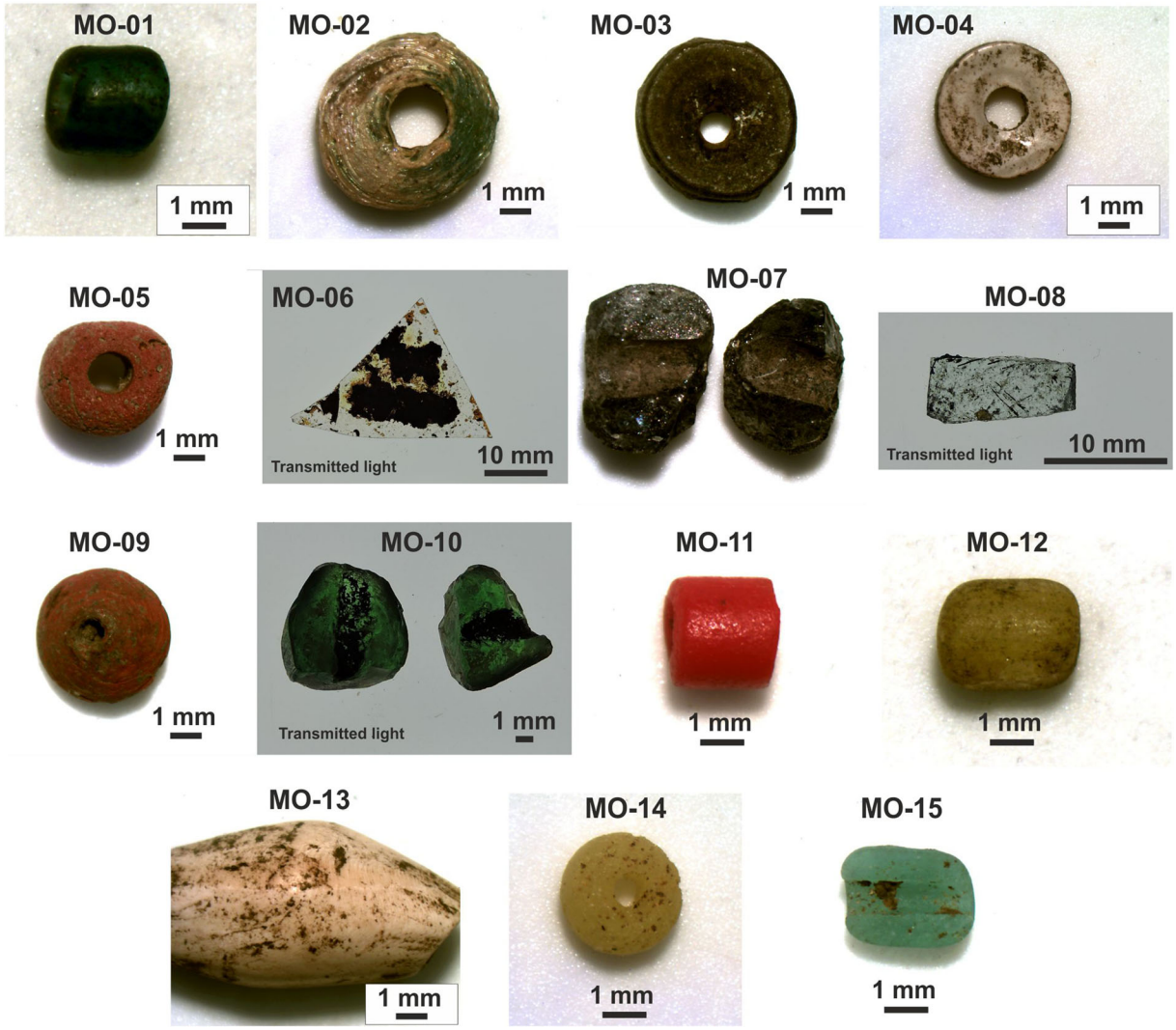

Fig. 4 Images of the samples studied as received in the lab

The brick red color and opacity of MO-09, on the contrary, are due to the presence of colloids or copper microcrystals (Cu^0, Cu^+) in the glass body, as shown in Fig. 6. It has an absorption band of about 550 nm that can be assigned to the presence of copper. In the chemical composition analysis, using EDS at low magnification, CuO was not detected (Fig. 7A, analysis 1). Therefore, higher magnifications were needed. It was only possible to observe such microcrystals at magnifications higher than × 10,000 (Fig. 7B, lighter points indicated with white arrows), generally smaller than 0.5 μm in size. In the corresponding EDS microanalysis (Fig. 7B, analysis 2 and 3), CuO was detected in varying proportions (1.5–3.3 wt. %). This suggests that the microcrystals of metallic copper or cuprous oxide (Cu_2O) of very small size (colloids) could be the chromophore responsible for this glass bead's red color and opacity. Based on these data, it can be suggested that this glass bead was made from the so-called copper hematinone glasses (Fernández Navarro 2003), which are opaque red glasses in which the reflection of light produces color in a more or less uniform dispersion of copper crystals (Cu^0, Cu^+) present in the glass body. Glasses that are colored by chromophores in a crystalline state, the so-called copper aventurine glasses (Fernández Navarro 2003), are well-known in the literature. However, the sample in this study is a copper hematinone glass. It differs from the aventurine in the size of microcrystals—approximately 0.5 μm in hematinone glass, which is smaller than in aventurine glasses by three orders of

Table 3 Chemical composition of glass samples obtained by EDS (wt. %)

Sample	Color	Oxides											Group
		Na_2O	MgO	Al_2O_3	SiO_2	Cl^-	K_2O	CaO	MnO	Fe_2O_3	ZnO	PbO	
MO-01	Bluish green	18.9	0.2	8.6	63.3	1.5	3.4	2.6	---	1.5	---	---	1. Mineral soda
MO-07	Opaque black	18.6	1.4	8.1	60.3	1.6	3.7	3.6	---	2.7	---	---	1. Mineral soda
MO-09	Opaque brick red	19.3	---	8.7	62.7	2.0	3.7	3.6	---	---	---	---	1. Mineral soda
MO-10	Green	21.0	---	7.8	62.4	0.9	2.6	1.8	---	3.5	---	---	1. Mineral soda
MO-12	Dark yellow	19.1	0.1	7.5	64.7	1.9	2.8	2.1	---	1.8	---	---	1. Mineral soda
MO-15	Greenish blue	21.0	---	8.9	62.0	1.7	3.3	1.7	---	1.5	---	---	1. Mineral soda
MO-02	Colorless greenish	18.0	4.7	5.0	64.2	1.3	2.6	3.8	---	0.4	---	---	2. Vegetal soda
MO-05	Opaque brick red	20.4	5.0	5.3	58.7	0.9	2.7	5.0	---	2.0	---	---	2. Vegetal soda
MO-06	Colorless (flat)	17.5	5.4	2.7	67.0	0.9	1.9	3.5	1.0	0.1	---	---	2. Vegetal soda
MO-14	Opaque yellow	16.7	5.2	4.9	58.7	1.0	3.0	4.2	---	0.5	---	5.8	2. Vegetal soda
MO-08	Bluish (flat)	15.3	---	3.0	71.6	1.2	---	9.0	---	---	---	---	3. Soda lime
MO-11	Opaque ruby red	20.1	---	---	67.6	---	4.3	---	---	---	8.0	---	Na_2O-ZnO-SiO_2

(—) not detected

magnitude. A smaller size of crystals occurs due to faster cooling of glass (Ahmed and Ashour 1981; Bamford 1977).

Plant-ash glasses from group 2 also showed a remarkable variety of chromophores and elaboration procedures, both ionic and colloidal. The colorless greenish color of MO-02 is likewise due to the presence of the Fe^{2+}/Fe^{3+} redox pair, whose chromatic sum results in a residual greenish appearance of the colorless glass given its relatively low Fe_2O_3 concentration (0.4 wt. %). In the MO-06 colorless glass sample, the presence of MnO (1.0 wt. %) suggests the use of manganese dioxide as decoloring agent (Green and Hart 1987).

The brick red color and opacity of MO-05, as in MO-09 mineral-soda glass, is also due to the colloids or copper microcrystals (Cu^0, Cu^+) in the glass body. Neither CuO was detected at low magnifications (Fig. 8A, analysis 1). At higher magnifications, microcrystals of a somewhat larger size of 0.5 μm, larger than those of the sample MO-09, could be observed (Fig. 8B, lighter points indicated with white arrows). In these points (Fig. 8C, analyses 2 and 3), CuO was detected in higher proportions (14.5–44.8 wt. %), which suggests that the chromophore responsible for the red color and opacity of this glass bead is also due to the microcrystals of metallic copper or cuprous oxide (Cu_2O), making this a copper hematinone glass (Fernández Navarro 2003).

The detection of PbO (5.8 wt. %, Table 3) in the body of the opaque yellow MO-14 glass bead suggested that its color was also probably due to the presence of colloids. High magnification observations of a polished cross-section resulted in identifying microcrystals between 5 and 10 μm in size (Fig. 9A–B). PbO and SnO_2 are mostly detected in these microcrystals (Fig. 9A, analysis 1; Fig. 9B, analysis 2), suggesting that the chromophore responsible for the yellow color and opacity of this glass is due to lead stannate. This lead-tin oxide is routinely identified in Islamic glazed ceramics (Salinas et al. 2019) and is also common in plant-ash glass beads from other sites in Sub-Saharan Africa (Robertshaw et al. 2010). The remarkable concentration of SiO_2 (8.4–15.1 wt. %) could indicate that type II lead stannate [$Pb(Sn,Si)O_3$] was used in producing this glass since type I lead stannate (Pb_2SnO_4) does not contain silicon oxide.

Moreover, although Fe_2O_3 was not detected in the glass body of MO-08 (Table 3), the bluish color of the single flat glass from group 3 is due to the presence of iron oxide and, specifically, to the higher intensity band of Fe^{2+}ions (blue) in comparison with bands at 380, 420, and 440 of Fe^{3+}ions (yellow) (Fig. 10). Finally, the opaque ruby red glass (MO-11), belonging to the Na_2O-ZnO-SiO_2 system, did not provide evidence of any ionic chromophore (Fig. 11A, analysis 1). Accordingly, a high magnification examination was undertaken to look for microcrystals. Some of the microcrystals identified (0.5–2.0 μm) can be observed in Fig. 11B. Apart from the prominence of Na_2O, K_2O, and SiO_2 in

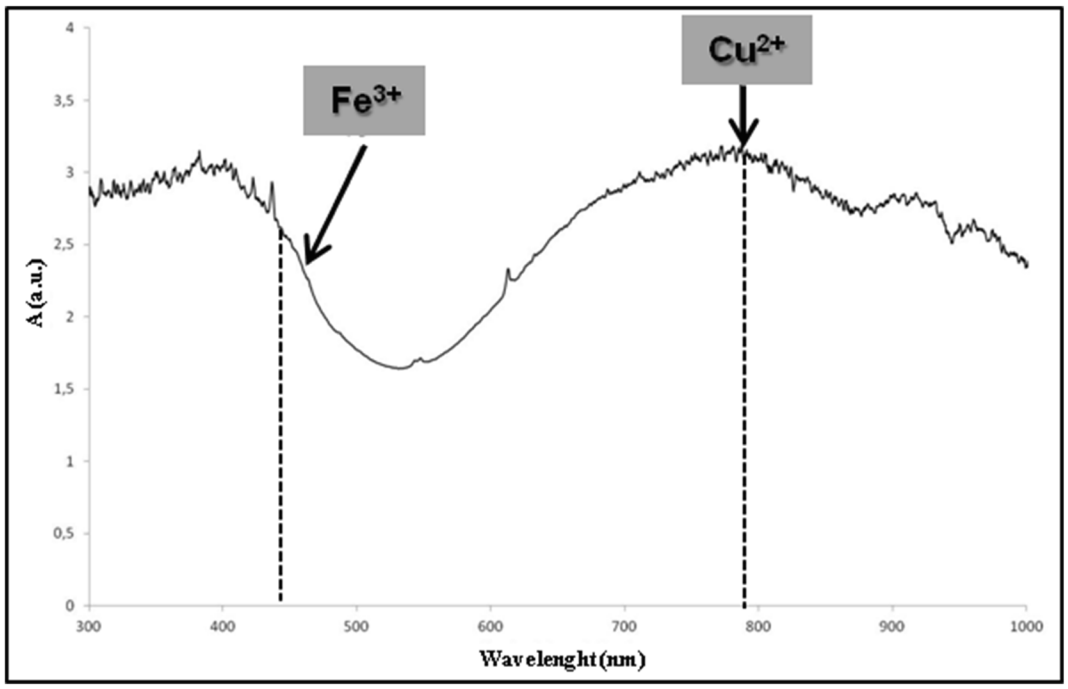

Fig. 5 Absorption spectrum from the MO-10 sample

the glass composition, a relatively high proportion of cadmium (41.0 wt. %), sulfur (11.0 wt. %), and selenium (7.6 wt. %) oxides are also detected in these microcrystals (Fig. 11B, analysis 2). The latter suggests that the chromophore responsible for this bead's red color and opacity is a dispersion of cadmium sulfoselenide microcrystals. In this case, the ruby color is favored by the presence of ZnO, whose optimum percentage in present-day glass production is between 8.0 and 10.0 wt. % (Fernández Navarro 2003). This fact agrees with

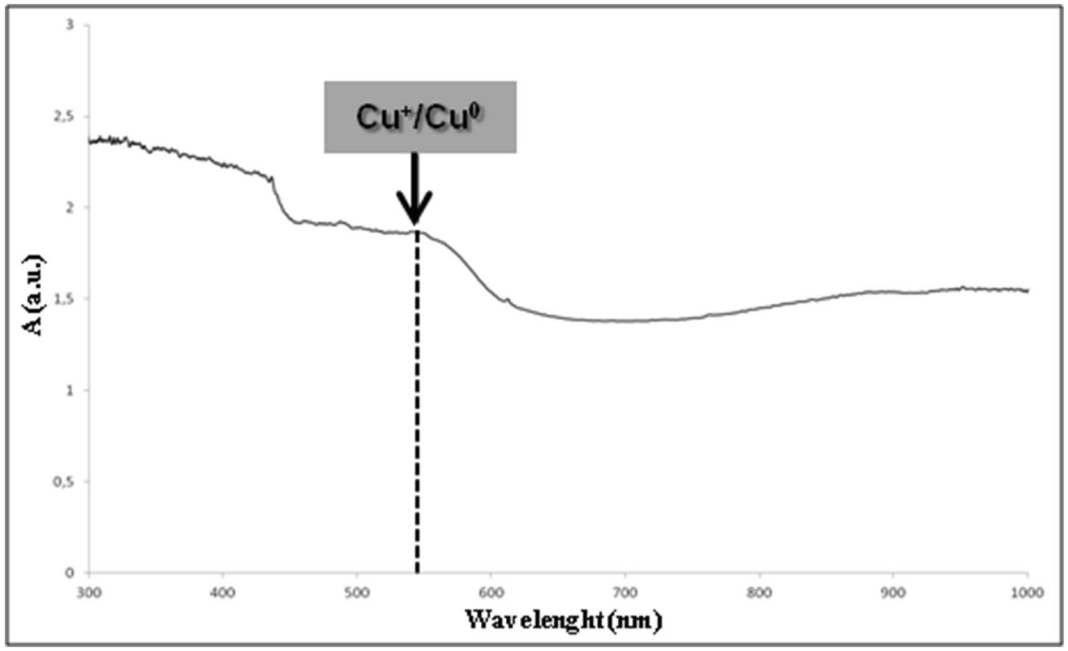

Fig. 6 Absorption spectrum from the MO-09 sample

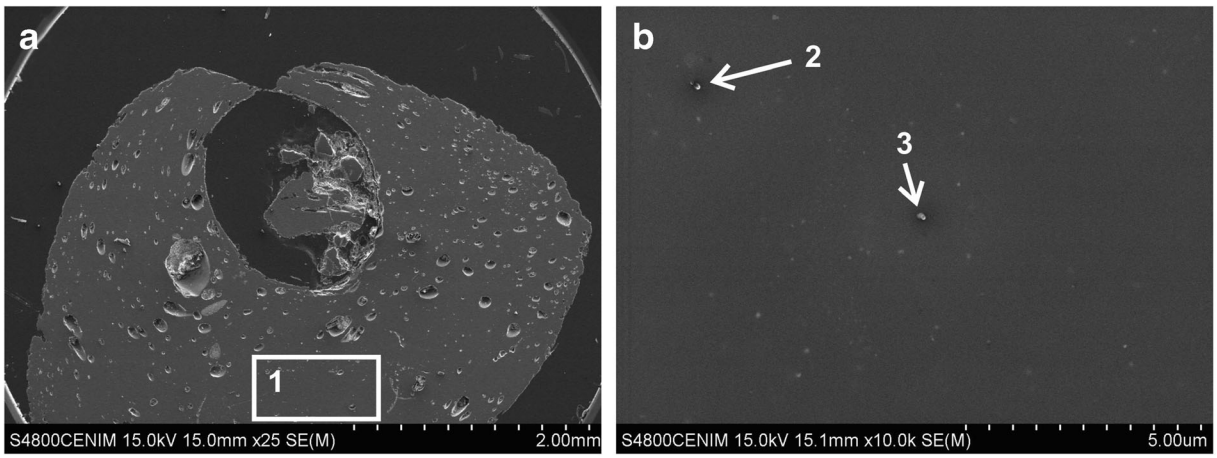

Analysis	Na_2O	MgO	Al_2O_3	SiO_2	Cl	K_2O	CaO	Fe_2O_3	CuO
1	14.6	---	7.1	63.6	2.0	4.0	3.8	4.9	---
2	11.7	---	7.9	69.4	1.3	2.6	2.4	3.2	1.5
3	13.5	---	7.8	66.8	1.6	2.1	2.0	2.9	3.3

Fig. 7 FESEM images from the MO-09 sample and places in which EDS microanalyses were undertaken. The table shows EDS results (wt. %). (—) not detected

the ZnO concentration detected in MO-11, which suggests a modern production of this sample. Ruby red glass beads, with the same morphology and presence of cadmium sulfoselenide as MO-11, have been found in other African sites in twentieth-century contexts, such as Magoro hill in South Africa (Prinsloo et al. 2012) and Kindoki in the Democratic Republic of the Congo (Coccato et al. 2017). However, no study provides data on glass compositions. Therefore, it is not possible to determine whether these ruby red beads were also elaborated from Na_2O-ZnO-SiO_2 glasses.

Shell and Fishbone Beads

The shell and fishbone beads were also analyzed for their chemical compositions (Table 4) to ascertain that what is observed as the beads' material makeup is consistent with chemical properties. Predictably, calcium and phosphorus showed the highest concentration in MO-03, which confirms that bone was used to make this bead since calcium phosphate [$Ca_3(PO_4)_2$] is the major inorganic component of a bone. Due to its morphology, it could be the vertebra of a fish. On the contrary, no

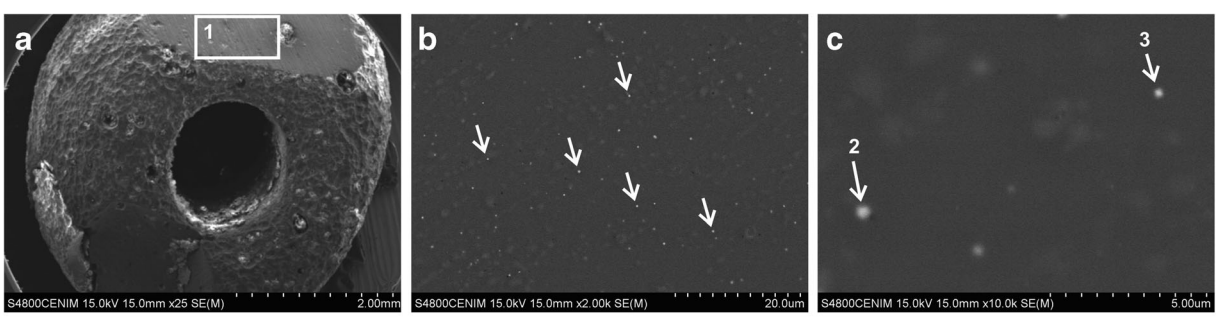

Analysis	Na_2O	MgO	Al_2O_3	SiO_2	Cl	K_2O	CaO	Fe_2O_3	CuO
1	20.5	4.9	5.0	59.0	0.8	2.4	5.5	1.9	---
2	11.7	2.9	3.3	32.6	0.4	1.0	2.2	1.1	44.8
3	13.1	3.5	4.7	53.7	0.8	2.6	4.9	2.2	14.5

Fig. 8 FESEM images from the MO-05 sample and places in which EDS microanalyses were undertaken. The table shows EDS results (wt. %). (—) not detected

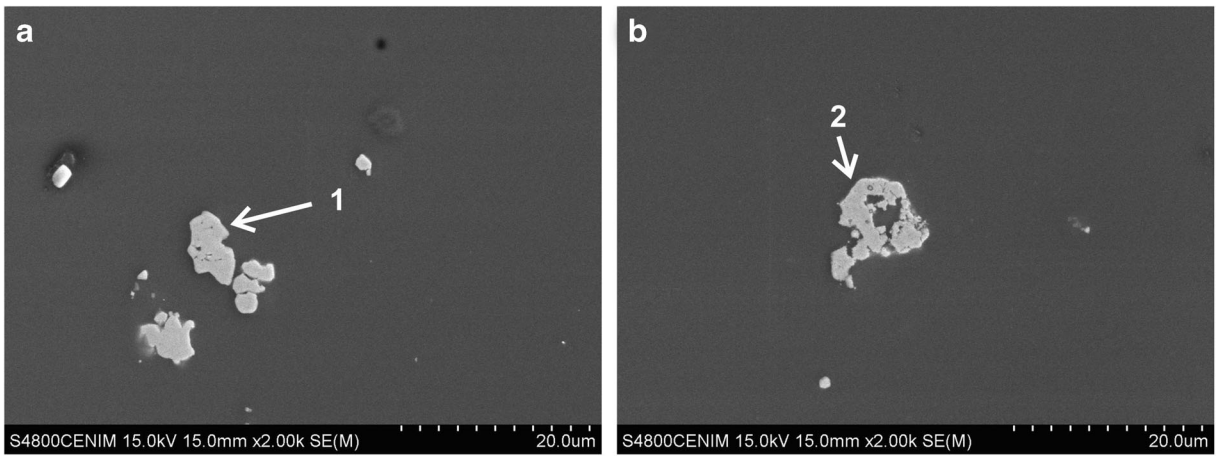

Analysis	Na_2O	MgO	Al_2O_3	SiO_2	SnO_2	PbO
1	4.5	1.5	1.9	15.1	25.6	51.4
2	---	---	---	8.4	31.8	59.8

Fig. 9 FESEM images from the MO-14 sample and places in which EDS microanalyses were undertaken. The table shows EDS results (wt. %). (—) not detected

phosphorus was detected in MO-04 and MO-13 but almost only calcium. This is also consistent with the expectation that these are shell beads. XRD analysis was used to look for crystalline phases in the samples. The X-ray diffractogram obtained for MO-04 (Fig. 12, left) indicates aragonite as the only crystalline phase present in the sample. The results confirmed that these beads were unequivocally made of shells since aragonite is

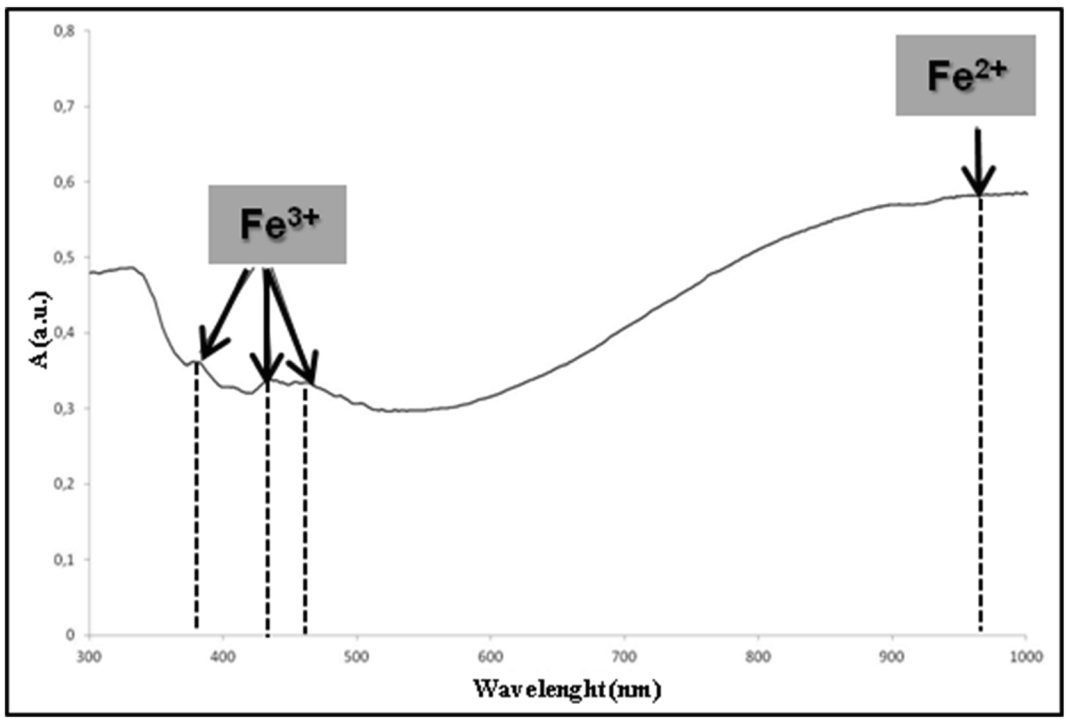

Fig. 10 Absorption spectrum from the MO-08 sample

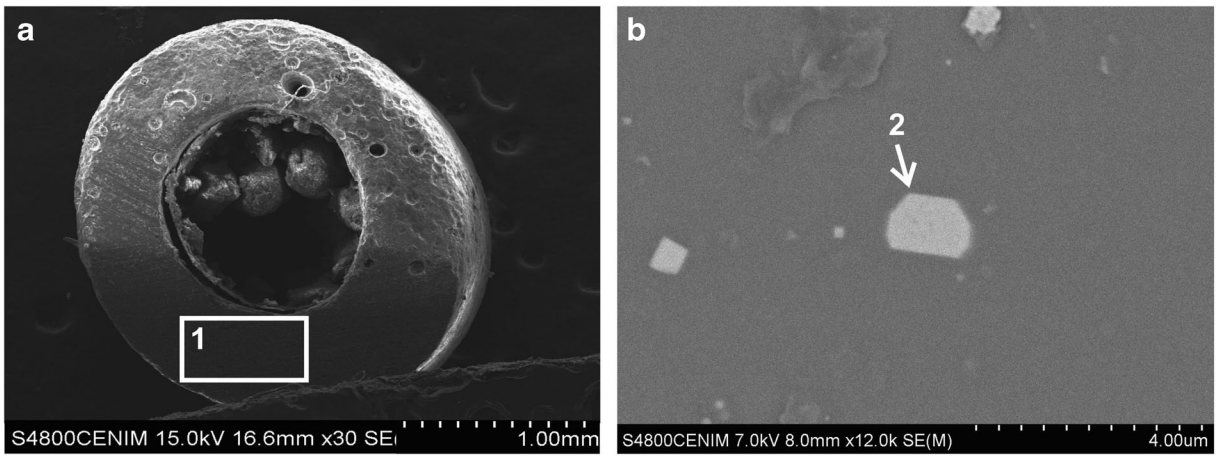

Analysis	Na_2O	SiO_2	SO_3	K_2O	ZnO	SeO_2	CdO
1	20.1	67.6	---	4.3	8.0	---	---
2	5.7	29.9	11.0	4.8	---	7.6	41.0

Fig. 11 FESEM images from the MO-11 sample and places in which EDS microanalyses were undertaken. The table shows EDS results (wt. %). (—) not detected

their main inorganic component. Given that many shell remains were recovered during excavation, it was decided to analyze one of the most abundant marine gastropod mollusks, *Lambis lambis* (spider conch) with XRD, for comparison. *Lambis lambis* is characterized by hollow digitations in the form of small horns that would have made it ideal as raw material for bead production (see white square of Fig. 12, right). Indeed, some tubular fragments compatible with part of these "horns" were recovered in several stratigraphic units of the C-400 site (Table 1). The resulting diffractogram of this gastropod sample (Fig. 12, center) revealed that it is also exclusively composed of aragonite, as in the shell beads. Consequently, it can be concluded that these beads were actually made by cutting small slices of shell hollow digitations from the local *Lambis lambis* gastropod mollusk.

Discussion

Eleven of the 12 glass samples were made from soda-lime silicate glass. This type of glass is technically very difficult to produce since a high temperature is needed. So far, the only evidence of primary glass production in Sub-Saharan Africa comes from the Yoruba city of Ile-Ife in southwest Nigeria, with a chronology of the eleventh through fifteenth century AD (Babalola et al. 2018). Also, the Garden Roller beads (K2 site, South Africa) are the only example of glass known to have been imported and then reworked in Sub-Saharan Africa (Wood 2011). There is no evidence of glass production or glass recycling on Ibo Island, in the Quirimbas archipelago, or in mainland Cabo Verde province. The most plausible possibility is that finished glass beads arrived on Ibo Island. Glass constitutes important evidence of

Table 4 Chemical composition obtained by EDS (wt. %) of beads made of shell and fishbone

Sample	Color	Material	Oxides							
			Na_2O	MgO	Al_2O_3	SiO_2	P_2O_5	K_2O	CaO	Fe_2O_3
MO-03	Black	Fishbone	0.9	1.3	14.8	24.0	20.8	1.1	33.9	3.2
MO-04	Light gray	Shell	---	---	---	1.3	---	---	98.7	---
MO-13	Pale ochre	Shell	1.6	0.6	---	1.7	---	1.5	94.6	---

(—) not detected

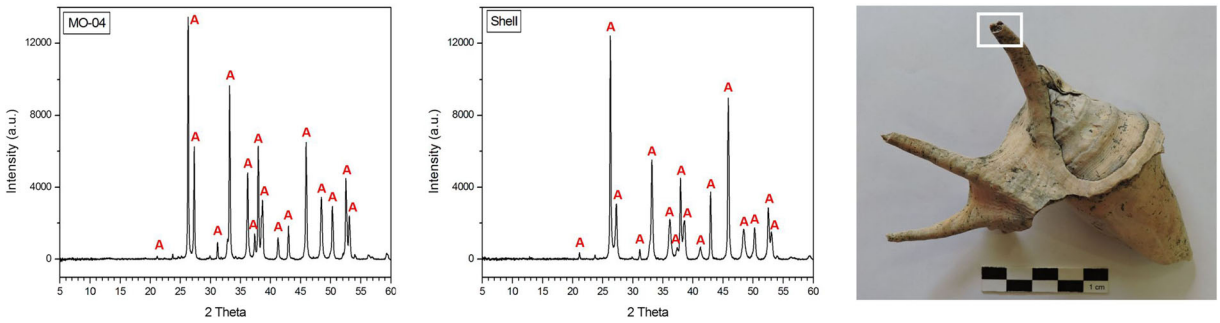

Fig. 12 X-ray diffractograms derived from the MO-04 sample (left) and the gastropod shell (center). Image of a gastropod shell (right) recovered in the C-400 site. A means Aragonite

long-distance trade, especially for understanding the directions of trade contacts between the Swahili communities of the Quirimbas and the northern coast of Mozambique. Along with shell beads, the glass could have served as currency for transactions with the inland communities (Wynne-Jonnes and Fleisher 2016).

The six glass beads of group 1 belong to the type of mineral-soda alumina glasses defined by Dussubieux et al. (2010) as m-Na-Al and first recognized in Indian glasses by Brill (1987). It is termed "m-Na" for an alkaline raw material of mineral origin and "Al" to indicate relatively high levels of Al_2O_3. There are five different groups of m-Na-Al glass, but only three of them: Groups 2, 4, and 5, were produced after the ninth century AD. Before the tenth century AD, only Group 1 was produced. Group 4 is known in Southeast Asia and Kenya from the fourteenth to the nineteenth centuries AD, while Group 5 is only identified at Sardis (Turkey) between the twelfth and fourteenth centuries AD. The m-Na-Al 2 group has been identified at sites on the west coast of India and the east coast of Africa dated from the ninth to the nineteenth centuries AD. The origin of the m-Na-Al 2 glass group, even though there is no evidence regarding where the workshops were located, has been placed somewhere on the western coast of India around sites such as the port of Chaul in the state of Maharashtra. Glass beads belonging to the m-Na-Al 2 group have been found in small quantities in South and Southeast Asia. However, they are abundant in East and southern African sites (Dussubieux et al. 2010; Robertshaw et al. 2010). This fact suggests that these glass beads were likely made for the African market. In addition, m-Na-Al 2 glass was commonly used for making beads, but it was never used to make vessels (Dussubieux et al. 2010).

Very recently, some new developments in glass chemistry have identified a new m-Na-Al 6 group. Instead of a large m-Na-Al 2 group covering the wide period from the ninth to the nineteenth centuries AD, there is now the m-Na-Al 6 group that widely circulated from the ninth to thirteenth centuries AD, while the m-Na-Al 2 group was prevalent from the fourteenth century onward. The m-Na-Al 6 group has been identified in eastern and southern Africa, and this group may have a west coast of India provenance based on the compositional similarities with the m-Na-Al 2 group (Seman et al. 2021).

The six glass beads of group 1 are related to m-Na-Al 2 glasses, as shown in Table 5. However, considering that site C-400 is dated to the eleventh and twelfth centuries, these beads are most likely associated with the new m-Na-Al 6 type of glasses. Although trace element analysis has not been conducted for the glass beads of group 1, the concentrations of oxides, such as MgO and CaO, are closer to average concentrations published for the m-Na-Al 6 group (MgO=0.3 for group 1 vs. 0.8 wt. % for m-Na-Al 6; CaO= 2.6 for group 1 vs. 2.5 wt. % for m-Na-Al 6, Seman et al. 2021, p. 92, table 1) than with average concentrations for the m-Na-Al 2 group (MgO=0.3 for group 1 vs. 1.2 wt. % for m-Na-Al 2; CaO= 2.6 for group 1 vs. 3.5 wt. % for m-Na-Al 2, Table 5).

The three beads and the colorless flat glass (MO-06) of group 2 belong to the type of plant-ash glasses in which the alkali source comes from ash obtained by burning halophytic plants. This type is characterized by relatively low concentrations of Al_2O_3, generally lower than 5.0 wt. %, and considered to be of Middle East origin (Brill 1995). The relatively low content of Al_2O_3 in the MO-06 sample (2.7 wt. %) matches the chemistry of published glass assemblages of Middle East origin, particularly from Nishapur. However, CaO concentrations are higher in the Middle East examples.

Table 5 Comparison of reduced chemical compositions (wt. %) for the six glass beads of group 1 (MO-01, MO-07, MO-09, MO-10, MO-12, MO-15) and data of the m-Na-Al 2 type from Dussubieux et al. (2010)

Oxides	Group 1		m-Na-Al 2	
	Mean	St. dev.	Mean	St. dev.
Na_2O	20.0	1.0	18.5	2.7
MgO	0.3	0.6	1.2	1.5
Al_2O_3	8.4	0.6	7.7	1.8
SiO_2	63.6	1.6	63.6	3.9
K_2O	3.3	0.5	2.4	0.9
CaO	2.6	0.9	3.5	0.9
Fe_2O_3	1.8	1.2	2.9	1.1

St. dev., standard deviation

The Al_2O_3 content, along with the presence of MnO as a decolorant agent, could suggest a Middle Eastern provenance for this flat glass shard since the MnO concentration in Islamic Middle Eastern glasses comprises 0.5 to 1.0 wt. % when used as decolorant (Brill 2001). On the contrary, the alumina contents of the other three glass bead samples are higher than 5.0 wt. %, which suggests that these samples belong to the vegetal-soda alumina glasses (v-Na-Al). It is termed "v-Na" for an alkaline raw material of vegetal origin and "Al" to indicate a relatively high level of Al_2O_3. In v-Na-Al glasses, alumina is commonly higher than 4.0 wt. %, while K_2O and MgO are always higher than 1.5 wt. %.

Until now, four types of v-Na-Al glass have been identified (Siu et al. 2020).

- Type A: found in glass beads from Mahilaka (Madagascar, thirteenth and fourteenth centuries, Robertshaw et al. 2006), Mapungubwe Oblate series beads (Zimbabwe Plateau, thirteenth and fourteenth centuries, Robertshaw et al. 2010), and Mambrui (Kenya, fifteenth and sixteenth centuries, Siu et al. 2020).
- Type B: identified in the Zimbabwean series of glass beads, fourteenth and fifteenth centuries (Robertshaw et al. 2010).
- Type C: identified in glass vessels from Mtwapa in Kenya, tenth through seventeenth centuries (Dussubieux and Kusimba 2012).
- Type D: found in glass vessels from Pengalan Bujang in Malaysia, twelfth and thirteenth centuries (Dussubieux and Allen 2014).

Of these four groups, only the first two were used to make glass beads.

The three glass beads of group 2 belong to the v-Na-Al type A glasses, used in the making of beads from the thirteenth to the sixteenth centuries. They are close in composition to Mahilaka glass beads but different from the Mapungubwe Oblate series and Mambrui glass beads, as illustrated in Table 6. This means that the Ibo Island beads are compositionally closer to the most ancient v-Na-Al glass beads of type A found in Mahilaka (thirteenth and fourteenth centuries), even though they appear in Ibo a little earlier (eleventh and twelfth centuries). The origin of the v-Na-Al glass beads of type A has been placed somewhere in Central Asia and could have reached the eastern coast of Africa via India (Siu et al. 2020). To summarize, the flat glass shard likely came from the Middle East, while the three beads possibly originated from Central Asia.

The single bluish glass sample (MO-08) of group 3 and the ruby red glass bead (MO-11) of the Na_2O-ZnO-SiO_2 system show compositional and technological features of refined raw materials. These two glass artifacts are, therefore, products of modern industrial processes. In the case of MO-08, it has contents of Na_2O (15.3 wt. %), CaO (9.0 wt. %), and SiO_2 (71.6 wt. %). There was no detection of MgO, K_2O, and Fe_2O_3. This chemical profile is similar to those of a conventional soda-lime silicate glass made with synthetic soda. The second case, MO-11, was produced from a glass in which CaO was replaced by ZnO as a stabilizer and colored from a colloidal chromophore of cadmium sulfoselenide. Accordingly, both cases could be products of modern European origin. Considering their small size and the sandy environment of the C-400 site, these modern glass samples must have percolated down from the upper levels.

As far as beads of shell and fishbone are concerned, those made from the vertebrae of fishbones only represent 1.25% of the bead assemblage. However, the shell beads of the *Lambis lambis* gastropod mollusk represent 38.75% of the total bead assemblage. The fishbone and shell beads were locally produced. This is proven by the tubular fragments of raw shells in several stratigraphic units of C-400 (Table 1, SU 401 and 404). Although no polishers were found in this unit, some fragments of polishers were recovered in two test pits (C-100 and C-300) located 150 m away from C-400, in the main square of the Ibo settlement. One of these polishers was found together with a shard of an imported glazed ware

of the Monochrome Yellow Sgrafiatto type in SU 104-3 of C-100 site (Priestman 2013, p. 593-94, plate 99). The sgraffito ware was made in south Iran (Fig. 13A, 13B). Two AMS dates from SU 104 (Fig. 13C–D) and the imported south Iran ware place the polisher between AD 995 and 1265. Another shard of an imported ware (Champlevé type) from south Iran of the same date was also found in the upper unit, SU 103-2 (Fig. 13E; Kennet 2004, p. 37; Priestman 2013, p. 585-586, plate 92). Even more interesting is the finding in SU 303-1 of a second polisher in C-300 (Fig. 13F), in association with some other beads made of glass and shell, as well as two beads made of gold and carnelian (Fig. 13G). The elemental composition of the gold bead is compatible with the Zimbabwean plateau (Ruiz-Gálvez et al. in press). An AMS short-life sample dated this unit to AD 971–1149 (Fig. 13H), suggesting a chronology of the late tenth to mid-twelfth century AD.

Most of the polishers and grinders found in Swahili sites are made from local shards, and their earliest appearance dated from AD 600. More than 3500 of these tools were excavated in domestic contexts at Tumbe (Pemba Island, Tanzania), seventh to tenth centuries AD (Flexner et al. 2008). In addition, the shell beads seem to have been made for local redistribution among the inland communities and could have been used as currency (Wynne-Jonnes and Fleisher 2016).

The excavation of C-400 provided data that suggests a probably short occupation, as evident by the single and coherent living floor. Five samples, three of them from terrestrial mammals and two from scapula of marine tortoises, were sent to Teledyne Direct AMS and Groningen laboratories for dating. Unfortunately, the terrestrial mammal bones did not preserve collagen or produced very old and incoherent dates. However, the two tortoise samples and imported ceramic wares provide a date range of the eleventh and twelfth centuries. This was the efflorescent period in the Swahili trade when the Red Sea superseded the Persian Gulf as the main commercial partner of Eastern Africa (Beaujard 2007). At this time, the Kilwa sultanate became dominant on the Swahili coast, controlling ivory and gold trade from Sofala in southern Mozambique, and expanded to Madagascar and the Comoros Islands. According to Horton (2004), some Indian traders and artisans were living in the African ports of the Indian Ocean at that time. The Indian artisans and traders were likely responsible for the carnelian bead found in the C-300 test pit mentioned above. This bead is similar to others found in Swahili centers such as Songo Mnara (Perkins et al. 2014) and Kilwa (Pollard and Kinyera 2017), both in Tanzania. Horton (2004) considers carnelian beads as either imported from India or locally made by Indian artisans due to the complex diamond tip drilling technique involved in their production. Therefore, group 1 (m-Na-Al 6) glass beads of the C-400 site reached the Ibo Island directly from south Asian sites through the Indian Ocean sea trade or indirectly through the Swahili entrepôts.

Wood et al. (2012) have discussed the geopolitical and commercial network shifts that created abrupt changes in the glass bead trade in southern Africa beginning in the mid-tenth century. These changes began when the Zhizo beads made with plant-ash glass (v-Na-Ca) were replaced by beads made with mineral soda glass thst has high alumina (m-Na-Al 6), known as K2 and East Coast Indo-Pacific series. These latter beads originated from the western coast of India. In the early thirteenth century, the Mapungubwe Oblate and then the Zimbabwe series made of v-Na-Al glass, whose provenance remains uncertain, replaced K2 and the East Coast Indo-Pacific series. In the mid-fifteenth century, Mapungubwe Oblate and Zimbabwe series were, in turn, replaced by Khami Indo-Pacific series (m-Na-Al 2), which also came from India. The K2 and East Coast Indo-Pacific series made of m-Na-Al 6 glasses are quite similar in composition to those of the group 1 glass beads from Ibo Island.

Except for Chibuene on the southern coast, no other site in Mozambique has been thoroughly excavated and published. The upper deposits (layer 100) of Chibuene, considered as a single latter occupation, have been dated to AD 1200-1700, while the lower deposits, the early occupation, are divided into two stratigraphic levels: layer 200 is dated to ca. AD 900–1200, and layer 300 to ca. AD 600–900 (Wood et al. 2012). According to the glass bead analysis at this site, there seems to be a gap between the late tenth and mid-fifteenth centuries. This is suggested by the fact that the K2 and East Coast Indo-Pacific series beads, made of m-Na-Al 6 (late tenth through the beginning of the thirteenth century), and the Mapungubwe Oblate and Zimbabwe series beads, made of v-Na-Al glass (thirteenth through mid-fifteenth centuries), were not found.

The only m-Na-Al glass identified at Chibuene is related to the Khami Indo-Pacific series dated to the mid-fifteenth century (Wood et al. 2012). In contrast, the Ibo C-400 site is dated to the eleventh and twelfth centuries and, therefore, it is not possible to compare the glass beads from Ibo Island with those found in

Table 6 Comparison of reduced chemical compositions (wt. %) for the three glass beads of group 2 (MO-02, MO-05, MO-14) and data from Mahilaka (Robertshaw et al. 2006), Mapungubwe Oblate series (Robertshaw et al. 2010) and Mambrui (Siu et al. 2020)

Oxides	Group 2		Mahilaka (Madagascar)		Map Oblate series (South Africa)		Mambrui (Kenya)	
	Mean	St. dev.	Mean	St. dev.	Mean	St. dev.	Mean	St. dev.
Na_2O	18.9	1.5	13.7	3.0	13.5	1.8	16.1	1.1
MgO	5.1	0.4	4.1	0.9	5.8	1.9	4.3	0.6
Al_2O_3	5.2	0.1	5.2	2.0	7.7	1.5	5.6	0.4
SiO_2	64.0	1.4	67.7	4.8	61.8	5.0		
K_2O	2.8	0.3	3.3	1.2	3.5	0.6	3.2	0.6
CaO	4.4	0.6	4.5	1.2	6.7	1.8	5.5	0.9
Fe_2O_3	1.0	0.9	1.4	1.2	1.0	0.3		

St. dev., standard deviation

Chibuene. Nonetheless, there are glass fragments in Chibuene belonging to eleventh-century Islamic perfume bottles (Ekblom and Sinclair 2018). The flat glass shard (MO-06) of group 2 from C-400 probably originated from these perfume bottles coming from the Middle East.

There is, however, a site located on Mayotte Island, one of the four islands in the Comoros archipelago and quite near the Quirimbas archipelago. This site is the necropolis of Antsiraka Boira, dated to the twelfth and thirteenth centuries (Fischbach et al. 2016). The glass beads unearthed in this necropolis almost have the same morphology as those of the Ibo C-400 site. Gastropod mollusks were also likely used to make the excavated shell beads because aragonite was identified in one of them. It is impossible to compare the chemical data of glass beads analyzed from this site since the authors only provide EDS results for five major oxides in which MgO was not detected. However, it seems that most of the glass beads from Antsiraka Boira belong to the K2 and the East Coast Indo-Pacific series and are related to the group 1 beads of C-400 on Ibo Island.

Both groups 1 (m-Na-Al 6) and 2 (v-Na-Al of type A) showed various chromophores and coloring procedures, both ionic and colloidal. In group 1, an ionic procedure due to the Fe^{2+}/Fe^{3+} ions redox equilibrium is responsible for the greenish-blue, dark yellow, and black colors, while bluish-green and green, apart from Fe^{2+}/Fe^{3+} ions, are due to the presence of Cu^{2+}ions. In addition, the brick red color is due to the presence of CuO_2 colloids and possibly originated from the so-called copper hematinone glasses. As far as group 2 is concerned, the colorless greenish cast is obtained with the Fe^{2+}/Fe^{3+} redox pair, whereas the colorless flat glass came from the use of manganese dioxide as decoloring agent. Brick red color is also obtained, as in group 1 glasses, by the presence of CuO_2 colloids. This indicates that copper hematinone glasses cannot be considered a technological distinction since they were produced in both mineral and vegetal-soda alumina glasses to get brick red beads. Moreover, the yellow color was obtained by lead stannate colloids. The presence of CuO_2 colloids in the hematinone glasses, of approximately 0.5 μm in size, proves the methodological advantage of using FESEM/EDS for characterizing these glasses against other chemical analysis techniques such as LA-ICP-MS. Due to the nano-scale and dispersion of CuO_2 microcrystals, the concentration of CuO could have been overestimated or underestimated if the LA-ICP-MS acquisition is undertaken on an area with or without the presence of such colloids. Although most of the glass beads from groups 1 and 2 showed superficial alterations, they presented an otherwise good state of conservation due to the higher chemical durability of soda-lime silicate glasses with a relatively high alumina content.

Conclusions

The glass, shell, and fishbone beads from Ibo Island's Swahili occupation level provide outstanding chemical composition data. The chemistry and chromophores of

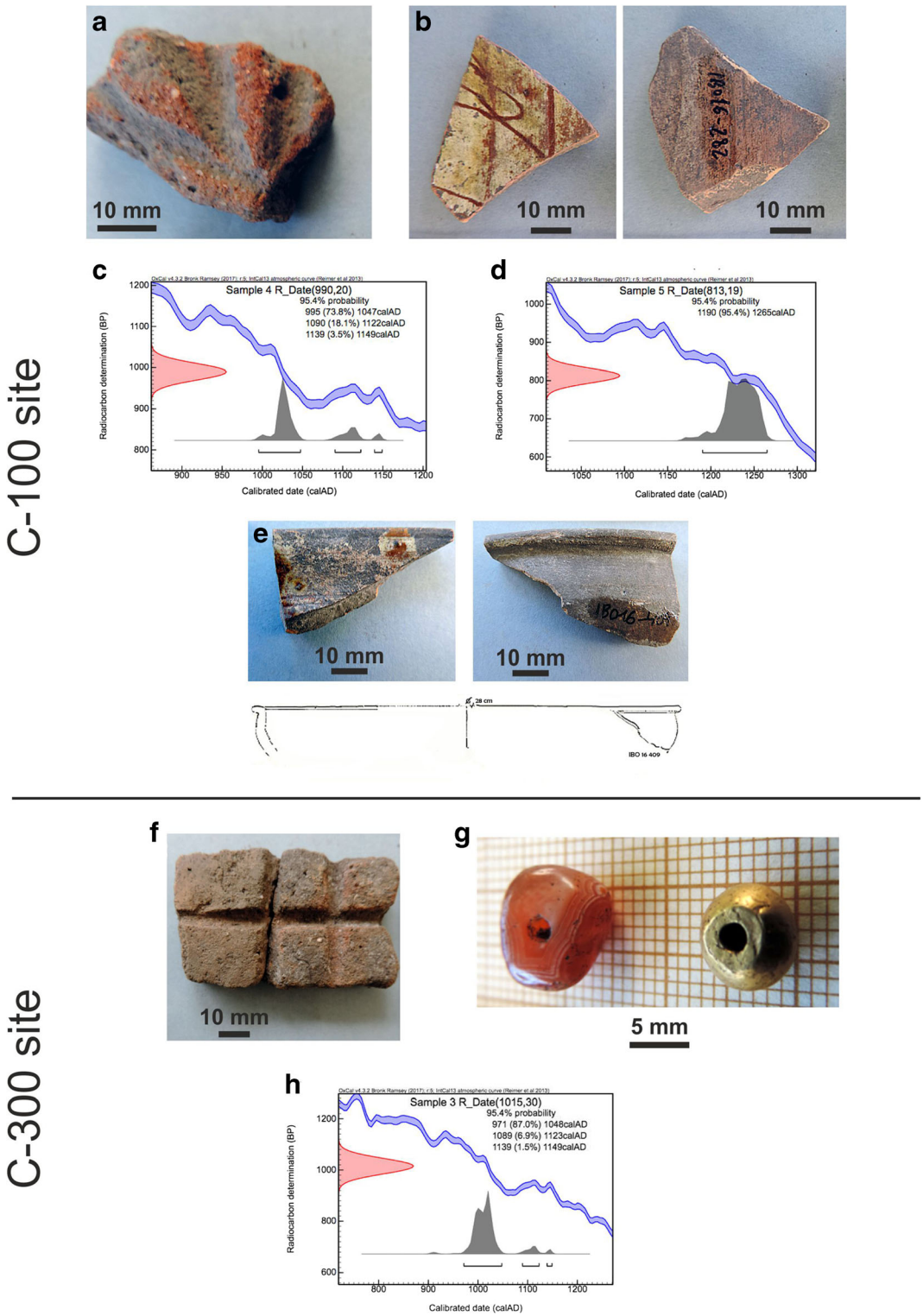

Fig. 13 Materials and AMS dates from C-100 and C-300 sites: (A) bead-polisher from the SU104-3; (B) imported shard from the SU104-3; (C–D) AMS dates from the SU 104; (E) imported shard from the SU 103-2; (F). bead-polisher from the SU 303-1; (G) carnelian and gold beads from the SU 303-1; (H) AMS date from the SU 303-1

the glass beads, in particular, give insights into aspects of the glass production techniques and provenance of the beads. The chemistry of the shell and fishbone beads provides an accurate determination of their material sources. Eleven of the 12 glass samples, including two shards of flat glass, were made from soda-lime silicate glass of the Na_2O-CaO-SiO_2 system, while one sample belongs to the Na_2O-ZnO-SiO_2 system in which ZnO replaced CaO as a stabilizer. The eleven soda-lime silicate glasses can be divided into three groups: mineral-soda alumina glasses (m-Na-Al), vegetal-soda alumina glasses (v-Na-Al), and conventional soda-lime silicate glass.

The glass beads on Ibo Island were imported. Beads belonging to the mineral-soda alumina glasses of group 1 seem to belong to the m-Na-Al 6 type, produced somewhere on the western coast of India and traded to the east coast of Africa from the ninth to the thirteenth century. Vegetal-soda alumina glasses of group 2 are related to v-Na-Al glass of type A identified in eastern and southern African sites from the thirteenth to the sixteenth century, even though it appears in the Ibo Island a little earlier, in the eleventh and twelfth centuries. The origin of the v-Na-Al glass beads of type A has been placed somewhere in Central Asia and could have reached the African east coast via India. A Middle East provenance is probable for the flat colorless glass shard, belonging to this group 2, due to its lower concentration of alumina and the presence of manganese dioxide used as decoloring agent. Both groups of glasses showed a variety of chromophores and coloring procedures, both ionic and colloidal. It should be highlighted that brick red color beads were produced from copper hematinone glasses due to the presence of CuO_2 colloids in both groups, while yellow color originated from microcrystals of lead stannate. These two groups of glasses are also present in other sites in East and southern Africa.

Group 3 only consists of a colorless bluish shard of flat glass. It has a chemical composition close to a conventional soda-lime silicate glass, which is likely of modern European production. A ruby red glass bead belongs to the Na_2O-ZnO-SiO_2 system, and this color was obtained from cadmium sulfoselenide colloids. Both glasses showed compositional and technological features characteristic of refined raw materials obtained by modern industrial processes. The shell beads made with *Lambis lambis* gastropod mollusk were locally produced and were meant for local redistribution. They could have been used as currency.

Supplementary Information The online version contains supplementary material available at https://doi.org/10.1007/s10437-021-09430-0.

Acknowledgements The authors acknowledge the financial support of the following programs and institutions: the Spanish Ministry of Economy, Industry, and Competitiveness through the National Program for Fostering Excellence in Scientific and Technical Research (Ref. HAR2013-48495-C2-2-P), the International Archaeological Excavations scheme from the Spanish Cultural Heritage Institute (IPCE), the Palarq Foundation, the program TOP Heritage: Technologies in Heritage Sciences from the Regional Government of Madrid (Ref. S2018/NMT-4372), and the Challenges of Society project from the Spanish Ministry of Science and Innovation (Ref. PID2019-104220RB-I00). Professional support from the TechnoHeritage network of Science and Technology for the Conservation of Cultural Heritage is also acknowledged. Some of the authors wish to acknowledge the professional support of the CSIC Interdisciplinary Thematic Platform, *Open Heritage: Research and Society* (PTI-PAIS).

Declarations

Conflict of Interest The authors declare no competing interests.

References

Adamowicz, L. (2011). Archaeological impact assessment for the proposed liquified natural gas project in Afungi and Cabo Delgado peninsulas, Palma district Cabo Delgado Province. Impacto Lda and Environmental Resources Management (ERM). Unpublished report. https://www.academia.edu/6543041. Accessed 24 September 2020.

Adamowicz, L. (2013). Levantamento arqueologico de salvaguarda na zona sul da Peninsula Afungi. Estudo do impacto ambiental da área pretendida pela Empresa Nacional de hidrocarbonetos-EP. Peninsula de Afungi, Dist. de Palma, Prov. de Cabo Delgado. Unpublished report. https://www.academia.edu/6543075. Accessed 24 September 2020.

Agua, F., Conde, J. F., Kobylińska, U., Kobyliński, Z., García-Heras, M., & Villegas, M. A. (2017). Chemical-physical characterization of Early Iron Age glass beads from Central Europe. *Boletín de la Sociedad Española de Cerámica y Vidrio, 56*(3), 119–130.

Ahmed, A. A., & Ashour, G. M. (1981). Effect of heat treatment on the crystallization of cuprous oxide in glass. *Glass Technology, 22*, 24–33.

Babalola, A. B., Dussubieux, L., McIntosh, S. K., & Rehren, T. (2018). Chemical analysis of glass beads from Igbo Olokun, Ile-Ife (SW Nigeria): New light on raw materials, production, and interregional interactions. *Journal of Archaeological Science, 90*, 92–105.

Bamford, C. R. (1977). *Colour generation and control in glass*. Amsterdam: Elsevier Scientific Publishing.

Bandenhorst, S., Sinclair, P., Ekblom, A., & Plug, I. (2011). Faunal remains from Chibuene, an Iron Age coastal trading station in Central Mozambique. *Southern African Humanities, 23*(1), 1–15.

Beaujard, P. (2007). East Africa, the Comoros Islands and Madagascar before the sixteenth century: On a neglected part of the world system. *Azania, 42*, 15–32.

Brill, R. H. (1987). Chemical analyses of some early Indian glasses. In H. C. Bhardwaj (Ed.), *Archaeometry of Glass. Proceedings of the Archaeometry Session of the XIV International Congress on Glass (1986 New Delhi, India)* (pp. 1–25, part I). Calcutta: Indian Ceramic Society.

Brill, R. H. (1995). Chemical analyses of some glass fragments from Nishapur in the Corning Museum of Glass. In J. Kröger (Ed.), *Nishapur: Glass of the early Islamic period* (pp. 211–233). New York: The Metropolitan Museum of Art.

Brill, R. H. (1999). *Chemical analyses of early glasses*. Corning, NY: The Corning Museum of Glass.

Brill, R. H. (2001). Some thoughts on the chemistry and technology of Islamic glass. In S. Carboni & D. Whitehouse (Eds.), *Glass of the Sultans* (pp. 25–45). New Haven, CT: Yale University Press.

Coccato, A., Costa, M., Rousaki, A., Bernard-Olivier, C., Karklins, K., Bostoen, K., Manhita, A., Cardoso, A., Barrocas, C., Candeias, A., Moens, L., Mirão, J., & Vandenabeele, P. (2017). Micro-Raman spectroscopy and complementary techniques (hXRF, VP-SEM-EDS, μ-FTIR and Py-GC/MS) applied to the study of beads from Kongo Kingdom (Democratic Republic of the Congo). *Journal of Raman Spectroscopy, 48*(11), 1468–1478.

de Torres, J., Ruiz-Gálvez, M. L., Fernández, V. M., Madiquida, H., & Mahumane, C. (2016). The Quirimbas Islands Project (Cabo Delgado, Mozambique): Report of the 2015 campaign. *Nyame Akuma, 85*, 57–68.

Duarte, R. T. (1993). *Northern Mozambique in the Swahili World: An archaeological approach*. Stockholm: Central Board of National Antiquities.

Duarte, R., & Meneses, P. (1996). The archaeology of Mozambique island. In G. Pwiti & R. Soper (Eds.), *Aspects of African archaeology. Papers from the 10th Congress of the Panafrican Association from Prehistory and Related Studies* (pp. 555–559). Harare: University of Zimbabwe Publications.

Dussubieux, L., & Allen, J. (2014). Chemical compositions of glass artifacts from Malaysia: New data from the sites of Kampung Pengkalan Bujang and Kampung Sungai Mas. In D. Perret & Z. B. Jaafar (Eds.), *Ancient glassware in Malaysia: The Pengkalan Bujang collection* (pp. 119–161). Kuala Lumpur: Department of Museums Malaysia.

Dussubieux, L., & Kusimba, C. M. (2012). Glass vessels in Sub-Saharan Africa: A compositional study of samples from Mtwapa, Kenya. In I. Liritzis & C. M. Stevenson (Eds.), *Obsidian and ancient manufactured glasses* (pp. 143–156). Albuquerque: University of New Mexico Press.

Dussubieux, L., Gratuze, B., & Blet-Lemarquand, M. (2010). Mineral soda alumina glass: Occurrence and meaning. *Journal of Archaeological Science, 37*(7), 1646–1655.

Ekblom, A., & Sinclair, P. J. J. (2018). Chibuene. In S. Wynne-Jones & A. LaViolette (Eds.), *The Swahili World* (pp. 175–181). London: Routledge.

Fernández Navarro, J. M. (2003). *El Vidrio. Constitución, fabricación, propiedades*. Madrid: CSIC 3rd edition.

Fischbach, N., Ngo, A.-T., Colomban, P., & Pauly, M. (2016). Beads excavated from *Antsiraka Boira* necropolis (Mayotte Island, 12th-13th centuries). Colouring agents and glass matrix composition comparison with contemporary Southern Africa sites. *ArcheoSciences-Revue d'archéométrie, 40*, 83–102.

Flexner, J. L., Fleisher, J. B., & LaViolette, A. (2008). Bead grinders and early Swahili household economy: Analysis of an assemblage from Tumbe, Pemba Island, Tanzania, 7th–10th centuries AD. *Journal of African Archaeology, 6*(2), 161–181.

García-Heras, M., Rincón, J. M., Jimeno, A., & Villegas, M. A. (2005). Pre-Roman coloured glass beads from the Iberian Peninsula: A chemico-physical characterization study. *Journal of Archaeological Science, 32*(5), 727–738.

García-Heras, M., Villegas, M. A., Agua, F., & Peña, J. (2019). *Caracterización y estudio arqueométrico de materiales cerámicos importados de un yacimiento Swahili de Mozambique*. Madrid: Instituto de Historia, CSIC, Internal report.

Green, L. R., & Hart, F. A. (1987). Colour and chemical composition in ancient glass: An examination of some Roman and Wealden glass by means of Ultraviolet-Visible-Infra-red Spectrometry and Electron Microprobe Analysis. *Journal of Archaeological Science, 14*, 271–282.

Henderson, J., McLoughlin, S. D., & McPhail, D. S. (2004). Radical changes in Islamic glass technology: Evidence for conservatism and experimentation with new glass recipes from early and middle Islamic Raqqa, Syria. *Archaeometry, 46*(3), 439–468.

Hill, D. V., Speakman, R. J., & Glascock, M. D. (2004). Chemical and mineralogical characterization of Sasanian and early Islamic glazed ceramics from Deh Luran Plain South Western Iran. *Archaeometry, 46*(4), 585–605.

Horton, M. (2004). Artisans, communities, and commodities: Medieval exchanges between Northwest India and East Africa. *Ars Orientalis, 34*, 62–80.

Kennet, D. (2004). *Sasanian and Islamic pottery from Ras-al-Khaimah: Classification, chronology and analysis of trade in the Western Indian Ocean. Oxford: Archaeopress, Society for Arabian Studies Monograph, 1*.

Koleini, F., Colomban, P., Pikirayi, I., & Prinsloo, L. C. (2019). Glass beads, markers of ancient trade in Sub-Saharan Africa: Methodology, state of the art and perspectives. *Heritage, 2*, 2343–2369.

Koleini, F., Colomban, P., & Pikirayi, I. (2020). Post-15th century European glass beads in southern Africa: Composition and classification using pXRF and Raman spectroscopy. *Journal of Archaeological Science: Reports, 29*(102183), 1–10.

Madiquida, H. (2007). *The iron-using communities of the Cape Delgado Coast from AD 1000*. Uppsala: Uppsala University, Studies in Global Archaeology 8.

Morais, J. M. (1988). *The early farming communities of Southern Mozambique*. Stockolm and Maputo: Central Board of National Antiquities of Sweden and Eduardo Mondlane University, Studies in African Archaeology 3.

Newitt, M. D. D. (1995). *A history of Mozambique*. Bloomington: Indiana University Press.

Palmer, H. C., & Newitt, M. D. D. (2016). *Northern Mozambique in the Nineteenth Century: The travels and explorations of H.E. O'Neill*. Leiden: Brill.

Perkins, J., Fleisher, J., & Wynne-Jones, S. (2014). A deposit of Kilwa-type coins from Songo Mnara, Tanzania. *Azania, 49*(1), 102–116.

Pollard, E., & Kinyera, O. C. (2017). The Swahili coast and the Indian Ocean trade patterns in the 7th-10th centuries CE. *Journal of Southern African Studies, 43*(5), 927–947.

Priestman, S. M. N. (2013). *A quantitative archaeological analysis of ceramic exchange in the Persian Gulf and Western Indian Ocean AD c.400-1275.* Ph.D. Thesis, Centre for Maritime Archaeology, University of Southampton, Southampton.

Prinsloo, L. C., Boeyens, J. C. A., van der Ryst, M. M., & Webb, G. (2012). Raman signatures of the modern pigment (Zn, Cd)$S_{1-x}Se_x$ and glass matrix of a red bead from Magoro Hill, an archaeological site in Limpopo Province, South Africa, recalibrate the settlement chronology. *Journal of Molecular Structure, 1023*, 123–127.

Robertshaw, P., Rasoarifetra, B., Wood, M., Melchiorre, E., Popelka-Filcoff, R. S., & Glascock, M. D. (2006). Chemical analysis of glass beads from Madagascar. *Journal of African Archaeology, 4*(1), 91–109.

Robertshaw, P., Wood, M., Melchiorre, E., Popelka-Filcoff, R. S., & Glascock, M. D. (2010). Southern African glass beads: Chemistry, glass sources and patterns of trade. *Journal of Archaeological Science, 37*(8), 1898–1912.

Ruiz-Gálvez, M. L. (2020). Comercio swahili en el norte de Mozambique. *Nailos. Estudios Interisciplinares de Arqueología Anejos, 6*, 103–133.

Ruiz-Gálvez, M. L., de Torres, J., & Fernández, V. M. (2017). The Swahili occupation of the Quirimbas (Northern Mozambique): The 2016 and 2017 field campaigns. *Nyame Akuma, 88*, 56–63.

Ruiz-Gálvez, M. L., Perea, A., Gutiérrez, C., Madiquida, H., de Torres, J., Fernández, V. M., & Mahumane, C. (in press). Qurimbas Islands (northern Mozambique) and the Swahili gold trade. *Journal of Archaeological Science: Reports*.

Salinas, E., Pradell, T., & Tite, M. (2019). Tracing the tin-opacified yellow glazed ceramics in the western Islamic world: The findings at Madinat al-Zahra. *Archaeological and Anthropological Sciences, 11*(3), 777–787.

Seman, S., Dussubieux, L., Cloquet, C., & Pryce, T. O. (2021). Strontium isotope analysis in ancient glass from south Asia using portable laser ablation sampling. *Archaeometry, 63*(1), 88–104.

Sinclair, P. J. J. (1985). *An archaeological survey of northern Mozambique (Part II: Cabo Delgado Province)*. Uppsala: Uppsala University, Working Papers in African Studies 12.

Sinclair, P. J. J. (1987). Um reconhecimento arqueológico do Norte de Moçambique: Provincia de Cabo Delgado. *Trabalhos de Arqueologia e Antropologia, 3*, 23–45.

Sinclair, P. J. J. (1991). Archaeology in eastern Africa: An overview of current chronological issues. *The Journal of African History, 32*(2), 179–219.

Sinclair, P. J. J., Nydolf, N. & Wickman-Nydolf, G. (1987). *Excavations at the University Campus Site 2532 Dc 1, Southern Mozambique.* Stockolm and Maputo: Central Board of National Antiquities of Sweden and Eduardo Mondlane University. Studies in African Archaeology 1.

Sinclair, P. J. J., Ekblom, A., & Wood, M. (2012). Trade and society on the south-east African coast in the later first millennium AD: The case of Chibuene. *Antiquity, 86*(333), 723–737.

Siu, I., Henderson, J., Qin, D., Ding, Y., Cui, J., & Ma, H. (2020). New light on plant ash glass found in Africa: Evidence for Indian Ocean Silk Road trade using major, minor, trace element and lead isotope analysis of glass from the 15th-16th century AD from Malindi and Mambrui, Kenya. *PLOS ONE, August, 13*, 1–26.

Wood, M. (2011). A glass bead sequence for southern Africa from the 8th to the 16th century AD. *Journal of African Archaeology, 9*(1), 67–84.

Wood, M. (2012). *Interconnections: Glass bead and trade in southern and eastern Africa and the Indian Ocean -7th to 16th centuries AD*. In *Studies in Global Archaeology 17*. Uppsala: Uppsala University.

Wood, M. (2018). Glass beads and Indian Ocean Trade. In S. Wynne-Jonnes & A. LaViolette (Eds.), *The Swahili World* (pp. 458–471). London & New York: Routledge.

Wood, M., Dussubieux, L., & Robertshaw, P. (2012). Glass finds from Chibuene, a 6th to 17th century AD port in southern Mozambique. *South African Archaeological Bulletin, 67*, 59–74.

Wynne-Jonnes, S., & Fleisher, J. (2016). Coins and other currencies on the Swahili coast. In C. Haselgrove & S. Krmnicek (Eds.), *The archaeology of money* (pp. 115–136). Leicester: Leicester University Press.

Wynne-Jonnes, S., & LaViolette, A. (2018). *The Swahili world*. London & New York: Routledge.